

# Shot-noise-driven escape in hysteretic Josephson junctions

J.P. Pekola,<sup>1</sup> T.E. Nieminen,<sup>1</sup> M. Meschke,<sup>1</sup> J.M. Kivioja,<sup>1</sup> A.O. Niskanen,<sup>1,2</sup> and J.J. Vartiainen<sup>1</sup>

<sup>1</sup>*Low Temperature Laboratory, Helsinki University of Technology, P.O. Box 3500, 02015 TKK, Finland*

<sup>2</sup>*VTT Information Technology, Microsensing, P.O. Box 1207, 02044 VTT, Finland*

We have measured the influence of shot noise on hysteretic Josephson junctions initially in macroscopic quantum tunnelling (MQT) regime. Escape threshold current into the resistive state decreases monotonically with increasing average current through the scattering conductor, which is another tunnel junction. Escape is predominantly determined by excitation due to the wide-band shot noise. This process is equivalent to thermal activation (TA) over the barrier at temperatures up to about four times above the critical temperature of the superconductor. The presented TA model is in excellent agreement with the experimental results.

Shot noise and full counting statistics (FCS) in mesoscopic conductors are currently intensively studied, because such measurements yield fingerprints of conduction mechanisms of these scatterers [1, 2, 3, 4]. Yet direct measurements of the second and higher moments of current or voltage are typically much more difficult and prone to errors as compared to the measurement of DC transport properties. This is because, in order to extract information about fluctuations, one generally needs to perform high frequency measurements on remotely connected samples at cryogenic temperatures, which is in practise a non-trivial task. Therefore, detectors of noise and FCS that operate directly on-chip near the noise source are of great importance. A recently proposed read-out device of these fluctuations is a Josephson junction (JJ) threshold detector [5, 6]. A mesoscopic non-hysteretic Josephson junction in the Coulomb blockade regime is another choice [7, 8, 9].

The dynamics of the JJ can be described as that of a phase ( $\varphi$ ) particle in a tilted cosine potential, see Fig. 1. Under the influence of equilibrium environment fluctuations at low temperatures the particle resides in the quantum mechanical ground state, from where the escape mechanism is tunnelling (MQT) through the barrier. At higher temperatures it assumes a nearly thermal population of the states, and the escape mechanism is predominantly thermal activation (TA) over the barrier top. Below we discuss the regime where excited states are not accessed by the influence of the thermal noise of the dissipative environment, which is an appropriate assumption based on our present measurements in the absence of shot noise and those of Ref. [10] in the same set-up at low temperatures.

The influence of noisy current on escape characteristics is typically considered in two different limits: (i) adiabatic (quasistationary) regime, where fluctuations of bias current that change the tilt of the cosine potential are so slow and weak that the phase particle remains in the ground state of the metastable well, and the escape rate is dictated by MQT from this varying ground state [6, 11], or (ii) (nearly) resonance excitation limit, where most of the escape events are consequences of shot-noise-

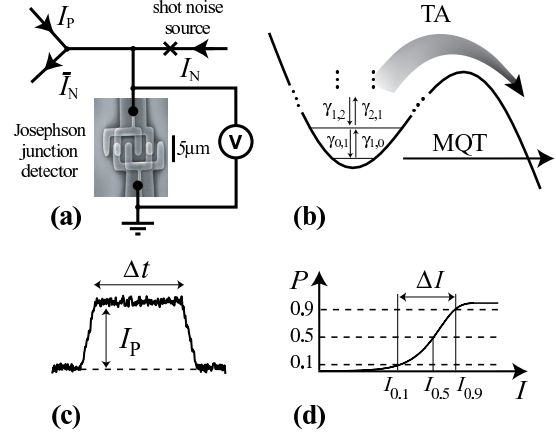


FIG. 1: (a) Measurement configuration. A split JJ in MQT regime measures the current fluctuations due to the shot noise of the scattering junction in the right arm. (b) Processes leading to escape from zero-voltage (supercurrent) state into resistive state. (c) Sketch of current pulses  $I_P$ , with superimposed noise of  $I_N$ , and (d) the associated escape characteristics. The central quantities relating to the pulses and escape histograms have been indicated in the figure.

driven excitations of the phase particle into higher levels in the well. Due to the high frequency resonance character of our on-chip circuit, it turns out that the latter approach is more appropriate in describing the dynamics of the detector in this case.

In this Letter we show that a hysteretic Josephson junction in MQT regime can measure high frequency current fluctuations generated by a mesoscopic scatterer in non-equilibrium. We present a model, in which the noisy current excites the phase particle in a metastable, nearly parabolic well out from the ground state, and subsequently the particle escapes from the well. This occurs via thermal activation at an equivalent temperature of the phase particle which is determined by the competition between shot-noise excitation, and relaxation due to the dissipative environment. This model is in excellent agreement with our experimental results, and we are able to investigate Josephson phase dynamics up to equivalent

temperatures which are about four times higher than the critical temperature of the superconductor. This is the temperature responsible for phase dynamics: the electrons and lattice of the superconductor are only weakly coupled to this subsystem, and the former two remain essentially at their base temperature.

Our measurement configuration with an electron micrograph of a split JJ detector is shown in Fig. 1. In a typical experiment two currents,  $I_N$  and  $I_P$ , are injected into the circuit through large resistances ( $> 1 \text{ M}\Omega$ ) at room temperature. Current  $I_N$  is applied constantly and it runs through another tunnel junction at a distance of  $120 \text{ }\mu\text{m}$  from the detector. This junction plays the role of the shot-noise source in the circuit. The DC-component of this current,  $\bar{I}_N$ , returns through a long (3 mm) and narrow (width  $2 \text{ }\mu\text{m}$ ) superconducting line such that no DC current due to  $I_N$  passes through the detector. We verify this balance frequently during the measurements. Thus, only the fluctuations of  $I_N$  are admitted through the detector. We probe these fluctuations by applying repeatedly trapezoidal current pulses of height  $I_P$  through the detector as shown in Fig. 1 (c). These pulses are slow, typically  $10 \text{ }\mu\text{s}$  -  $10 \text{ ms}$  long and with long transient times at the beginning and at the end of the pulse to secure adiabatic response to them. Typically 1000 pulses at each value of  $I_P$  are repeated, and the escape probability  $P(I_P)$  is obtained as the fraction of those pulses that lead to escape from the supercurrent state.

Let us discuss the dynamics of a hysteretic JJ in more detail. In the common RCSJ-model (Resistively and Capacitively Shunted Junction model), the phase particle in the tilted cosine potential is either trapped and oscillating in one of the wells, or alternatively it runs down the potential. The latter regime is called resistive state. The measurable quantities, *i.e.*, current  $I$  and voltage  $V$ , are related to  $\varphi$  via the Josephson equations:  $I = I_C \sin \varphi$  and  $2eV = \hbar \frac{d\varphi}{dt}$ , where  $I_C = \frac{2e}{\hbar} E_J$  is the critical current of the junction and  $E_J$  is its Josephson coupling energy. The quality factor  $Q \equiv \omega_p RC$  is assumed to be  $Q \gg 1$  to assure hysteretic dynamics. This means that once the particle leaves the well, it runs freely such that the voltage across the junction is close to twice the energy gap of the superconductor, and it can be retrapped to the zero-voltage supercurrent state only when current is lowered virtually to zero. Here  $R$  is the resistive shunt of the junction,  $C$  is the parallel capacitance, and  $\omega_p \equiv \sqrt{8E_J E_C q_0}/\hbar$  is the plasma frequency, where  $E_C = e^2/2C$  and  $q_0 = \sqrt{2(1 - I/I_C)}$ . Quantum mechanically the phase particle has energy states in the nearly parabolic wells, with energies close to those of a harmonic oscillator:  $E_n \simeq (n + 1/2)\hbar\omega_p$ .

Due to the nearly harmonic potential, transitions between the neighbouring levels are dominating. The rates of these transitions, see Fig. 1 (b), are determined by the spectral density  $S_I(\omega) = \int_{-\infty}^{\infty} \langle I(t)I(0) \rangle \exp(i\omega t) dt$  of the current noise at the corresponding level separation

$\omega = \omega_{j,j-1}$  as  $\gamma_{j,j-1} \simeq (j/2\hbar\omega_{j,j-1}C)S_I(-\omega_{j,j-1})$  and  $\gamma_{j-1,j} \simeq (j/2\hbar\omega_{j,j-1}C)S_I(+\omega_{j,j-1})$  for excitation and relaxation, respectively [7, 13]. The noise spectrum has two contributions, one due to the equilibrium environment,  $S_I^{\text{env}}$ , and the other due to shot noise,  $S_I^{\text{shot}}$ , which add incoherently:  $S_I = S_I^{\text{env}} + S_I^{\text{shot}}$ . At low temperature,  $k_B T \ll \hbar\omega_p$ , the thermal excitation is strongly suppressed,  $S_I^{\text{env}}(-\omega_{j,j-1}) \rightarrow 0$ , and the relaxation is due to zero point fluctuations,  $S_I^{\text{env}}(+\omega_{j,j-1}) \rightarrow 2\hbar\omega_{j,j-1}\text{Re}Y(\omega_{j,j-1})$ , where  $Y(\omega)$  is the admittance of the circuit surrounding the Josephson junction. The shot noise responsible for transitions in the Josephson junction can be described as  $S_I^{\text{shot}}(\pm\omega_{j,j-1}) = Fe\bar{I}_N$ . Here  $\bar{I}_N$  is the average current through the scatterer, and  $F$  is the "Fano factor" of the noise source and the circuit surrounding the JJ, at the frequency corresponding to level separation. Factor  $F$  can be calculated for a known experimental circuit. Here we determine it experimentally as a fit parameter. It would be unity in the case of Poissonian tunnel junction source [1] and if all the noise current would run through the detector junction. Combining the results above, we have

$$\gamma_{j,j-1} \simeq \frac{jFe\bar{I}_N}{2\hbar\omega_{j,j-1}C} \quad (1)$$

and

$$\gamma_{j-1,j} \simeq \frac{jFe\bar{I}_N}{2\hbar\omega_{j,j-1}C} + \frac{j\omega_{j,j-1}}{Q}. \quad (2)$$

The level dynamics described by Eqs. (1) and (2) can be described by the equivalent temperature  $T^*$  and effective quality factor  $Q^*$  by requesting  $\gamma_{j,j-1} \equiv j\frac{\omega_{j,j-1}}{2Q^*}[\coth(\hbar\omega_{j,j-1}/2k_B T^*) - 1]$  and  $\gamma_{j-1,j} \equiv j\frac{\omega_{j,j-1}}{2Q^*}[\coth(\hbar\omega_{j,j-1}/2k_B T^*) + 1]$ . This yields  $Q^* = Q$  and, with  $\omega_{j,j-1} \simeq \omega_p$

$$k_B T^* \simeq \frac{\hbar\omega_p}{2\text{arccoth}(1 + QFe\bar{I}_N/\hbar\omega_p^2 C)}. \quad (3)$$

Following the standard results of the decay from a cubic metastable well, we can infer that thermal activation is the dominant escape mechanism provided  $T^* > T_0 \equiv \hbar\omega_p/2\pi k_B$ . This yields a condition for the validity of the TA model:  $\text{arccoth}(1 + QFe\bar{I}_N/\hbar\omega_p^2 C)/\pi < 1$ . This is fulfilled at all currents  $\bar{I}_N$  that were employed in the experiments, as we will show below. With this procedure it is then straightforward to obtain the switching probability of the threshold detector, in the limit of many levels in the well, as  $P(\bar{I}_P) = 1 - \exp(-\Gamma\Delta t)$ . Here  $\Gamma = \frac{\omega_p}{2\pi} \exp(-\Delta U/k_B T^*)$  is the standard TA escape rate,  $\Delta t$  is the length of the current pulse, and  $\Delta U = 4\sqrt{2}E_J(1 - I_P/I_C)^{3/2}/3$  is the height of the potential barrier at the particular bias point  $I_P$ . The expressions above allow us to evaluate the position  $I_{0.5}$  and the width  $\Delta I = I_{0.9} - I_{0.1}$  of the escape threshold, where

TABLE I: Parameters of the two samples.

Sample	$I_C$ detector	$C$ detector	$I_C$ scatterer	$C$ scatterer
A	$3.9 \mu\text{A}$	230 fF	600 nA	40 fF
B	$1.5 \mu\text{A}$	230 fF	15 nA (1) 90 nA (2)	10 fF (1) 40 fF (2)

$I_x$  is defined by  $P(I_x) \equiv x$ , see Fig. 1 (d). These approximate results were compared to those obtained by full level dynamics calculation [12] numerically. They were identical, although there the results depended sensitively on the exact values of the level positions and widths near the barrier top.

In the limit of large noise currents,  $\bar{I}_N \gg \frac{\hbar\omega_p^2 C}{QFe}$ , we obtain  $T^* \simeq \frac{QFe\bar{I}_N}{2k_B\omega_p C}$ , which can be written in a more familiar looking form  $T^* \simeq \frac{Fe\bar{I}_N}{2k_B/R}$ . This is a valid approximation in a wide range of experimental parameters. The expressions of TA escape and the current dependence of the barrier height combined with this approximate expression of  $T^*$  finally allow us to approximate  $I_{0.5}$  and  $\Delta I$  as

$$I_{0.5}/I_C \simeq 1 - \left(\frac{3}{4\sqrt{2}}\right)^{2/3} \left[\ln\left(\frac{\omega_p \Delta t}{2\pi\kappa_{0.5}}\right)\right]^{2/3} \left(QF \frac{E_C}{E_J} \frac{\bar{I}_N}{e\omega_p}\right)^{2/3} \quad (4)$$

and, further assuming  $\omega_p \Delta t \gg 1$  yields

$$\Delta I/I_C \simeq \frac{\ln(\kappa_{0.9}) - \ln(\kappa_{0.1})}{[12 \ln(\frac{\omega_p \Delta t}{2\pi})]^{1/3}} \left(QF \frac{E_C}{E_J} \frac{\bar{I}_N}{e\omega_p}\right)^{2/3}. \quad (5)$$

Here  $\kappa_x \equiv -\ln(1-x)$ .

We report on data of two samples, A and B, which were fabricated by standard electron beam lithography and shadow evaporation with aluminium as the superconductor. The samples were measured via adequately filtered signal lines in dilution refrigerators at bath temperatures of 30 mK - 1 K. Sample A had a split JJ detector and one scattering junction as in the scheme of Fig. 1. Sample B had a single JJ as a detector, and it had two scattering junctions located symmetrically with respect to the detector (at a distance of 120  $\mu\text{m}$ ), and with respect to two long injection lines. In this sample the two scattering junctions were made intentionally very different to check the invariance of the results with respect to junction properties. The parameters of the two samples are listed in Table I.

Data in Fig. 2 (a) show results of a control experiment on Sample B at the base temperature  $T \simeq 30$  mK, where the trapezoidal pulse current  $I$  was injected through (i) one of the long injection lines, (ii) through scatterer 1, and (iii) through scatterer 2. The histogram of case (i) lies at higher currents than those of (ii) and (iii), which in turn overlap practically with each other. This

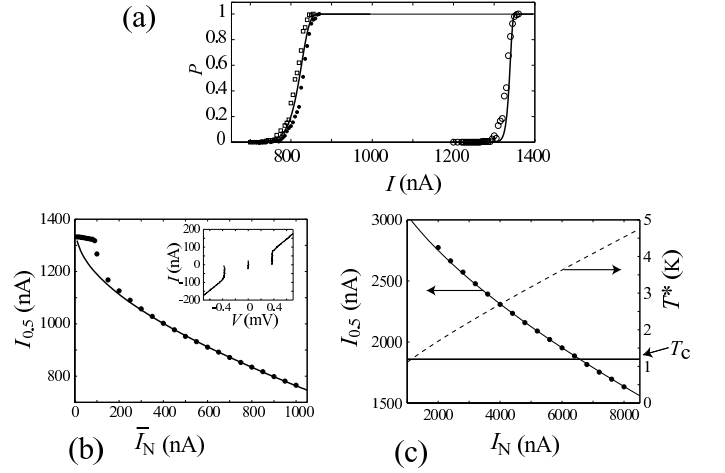


FIG. 2: Histogram positions under shot noise injection. (a) Escape histograms of Sample B when 800  $\mu\text{s}$  long current pulses have been injected through the long injection line (open circles), and through the two noise sources (1 - squares, 2 - filled circles), respectively. The lines are the corresponding theoretical results. (b) Experimental results (circles) on the switching threshold current  $I_{0.5}$  against the average current  $\bar{I}_N$  through the scatterer 2 in Sample B. Pulse length was  $\Delta t = 800 \mu\text{s}$ . The solid line is again the result of the used theoretical model. The inset shows the  $IV$  curve of the noise source. (c) Similar data as in (b) but for Sample A. The rising curve shows the corresponding equivalent temperature  $T^*$ , which ranges from 2 to 5 K in this measurement.

demonstrates that shot noise tends to push the threshold towards lower values of current, as predicted, *e.g.*, by Eq. (4). Furthermore these data demonstrate that the noise is predominantly, and equally in (ii) and (iii), generated by the scattering tunnel junctions. The calculated lines run through the corresponding experimental histograms assuming MQT without any noise in (i) and TA with  $T^*$  evaluated from Eq. (3) with  $QF = 5$  in (ii) and (iii). The latter value is realistic in terms of the expected  $Q \simeq 10$  [10] and  $F \leq 1$ .

Figure 2 (b) shows data on Sample B at the temperature  $T = 40$  mK. The threshold current  $I_{0.5}$ , *i.e.*, the pulse current at which the switching probability is 50%, has been plotted as a function of  $\bar{I}_N$  through the scatterer (2). The data, shown by solid symbols, follow the prediction of the model presented above, again with  $QF = 5$ . The initial plateau in the experimental data below  $I_N \simeq 100$  nA arises because the scattering junction is not in the linear quasiparticle tunnelling regime here. The inset of Fig. 2 (b) shows the  $IV$  curve of this junction.

In Fig. 2 (c) we plot, in addition to similar data as in (b), the equivalent temperature  $T^*$  in the measurement of Sample A when current  $\bar{I}_N$  is varied between 2  $\mu\text{A}$  and 8  $\mu\text{A}$ . There are two interesting points to note. (i) We are able to study Josephson dynamics of the JJ up

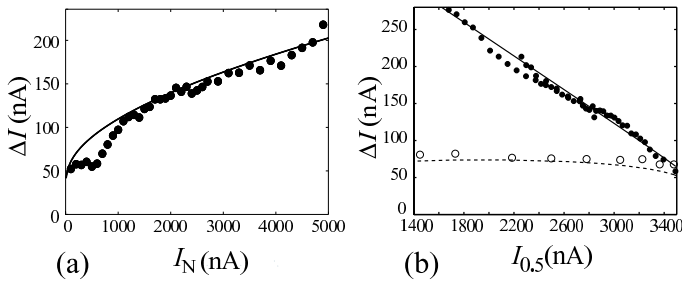


FIG. 3: The width of the histograms when shot noise and thermal noise are applied. (a) The width of the grey zone,  $\Delta I$ , against the average current  $\bar{I}_N$  through the scatterer. The dots are the experimental results and the solid line is the result of the theoretical model. (b)  $\Delta I$  vs.  $I_{0.5}$  under two different experimental conditions. The filled circles are data with elevated shot-noise temperature  $T^*$ , whereas the open circles are with variable bath temperature  $T$ . The solid line is the result of thermal activation model with constant energy gap, and the dashed line takes into account the suppression of the BCS gap [14] in the measurement with increased  $T$ .

to temperatures  $T^* \simeq 5$  K, about four times above the critical temperature  $T_C$  of aluminium. (ii) At all currents employed we are well above the threshold  $I_0$  of thermal activation: for this particular sample  $I_0 \simeq 0.3$  K.

Figure 3 (a) shows the width of the switching threshold,  $\Delta I$ , of sample A. Again the experimental (circles) and theoretical (line) results are in good agreement between each other using the same fit parameters as in Fig. 2. In Fig. 3 (b) data on switching of Sample A has been plotted in two different experimental conditions, in each case as  $\Delta I$  vs.  $I_{0.5}$ . The open circles are data where the bath (lattice) temperature has been varied by heating the sample stage to several temperatures  $T$  in the range 0.03 - 1 K. The full circles are data taken at the base temperature of the cryostat ( $T \simeq 30$  mK), but by varying the equivalent temperature  $T^*$  injecting different levels of  $\bar{I}_N$ . The line closely following the latter data is that originating from the thermal activation model. At the first sight it is surprising that the truly thermal data (open circles) fall far below this line and the other set of data. This is, however, accounted for by the fact that when increasing the bath temperature close to  $T_C$  of aluminium ( $\sim 1.2$  K), the BCS energy gap is progressively diminishing, thus leading to decrease of the critical current. The line following closely this data set is obtained by using the very same thermal activation model, but by taking into account suppression of the BCS gap due to temperature  $T$  [14]. This figure thus demonstrates that our thermal activation model is in good agreement with the shot noise data, and that it is indeed possible, by promoting shot noise, to study Josephson dynamics at super- $T_C$  temperatures without suppressing superconductivity.

Finally there are a few more topics to address. We found out that the adiabatic models of rocking slowly the current bias of the JJ do not account for our observations on shot noise: the adiabatic models, involving no excitations, predict exponential dependence in variance-of-the-current of the tunnelling rate from the ground state through the barrier [6, 11]. Our experimental results demonstrate, however, much weaker dependence, which we derived in this Letter. The (nearly) resonant model works in this case because the circuit responding to the shot noise resonates at frequencies, which are of the same order as the plasma frequency of the junction. Furthermore, the low frequency noise does not run through the detector junction but rather leaks through the bias line. Note that at DC we suppress the detector current due to  $I_N$  totally. The second issue is the assessment of an MQT detector as an absolute noise detector. Based on the invariance of the obtained results, especially in terms of results on different scatterers on the same sample, see Fig. 2 (a), we suggest that this kind of a detector could be made into an absolute on-chip detector of Fano-factors [1], and noise in general, by careful tailoring of the circuit surrounding the JJ and by measuring  $Q$  independently.

We thank T. Heikkilä, T. Ojanen, E. Sonin and A. Savin for useful discussions, and H. Grabert and D. Esteve for their insightful comments at an early stage of this work. We acknowledge Academy of Finland for financial support.

- 
- [1] Y.M. Blanter and M. Büttiker, *Physics Reports* **336**, 1 (2000).
  - [2] *Quantum Noise in Mesoscopic Physics*, edited by Yu.V. Nazarov (Kluwer, Dordrecht, 2003).
  - [3] L.S. Levitov, H.W. Lee, and G.B. Lesovik, *J. Math. Phys.* **37**, 4845 (1996).
  - [4] B. Reulet, J. Senzier, and D.E. Prober, *Phys. Rev. Lett.* **91**, 196601 (2003); B. Reulet, L. Spietz, C.M. Wilson, J. Senzier, and D.E. Prober, cond-mat/0403437.
  - [5] J. Tobiska and Yu.V. Nazarov, *Phys. Rev. Lett.* **93**, 106801 (2004).
  - [6] J.P. Pekola, *Phys. Rev. Lett.* **93**, 206601 (2004).
  - [7] R.J. Schoelkopf, A.A. Clerk, S.M. Girvin, K.W. Lehnert, and M.H. Devoret, in Ref. [2].
  - [8] R.K. Lindell *et al.*, *Phys. Rev. Lett.* **93**, 197002 (2004).
  - [9] T.T. Heikkilä, P. Virtanen, G. Johansson, and F.K. Wilhelm, *Phys. Rev. Lett.* **93**, 247005 (2004).
  - [10] J.M. Kivioja *et al.*, cond-mat/0501383.
  - [11] J.M. Martinis and H. Grabert, *Phys. Rev. B* **38**, 2371 (1988).
  - [12] A.I. Larkin and Yu.N. Ovchinnikov, *Zh. Eksp. Teor. Fiz.* **91**, 318 (1986); *Sov. Phys. JETP* **64**, 185 (1987).
  - [13] J.M. Martinis, S. Nam, J. Aumentado, K.M. Lang, and C. Urbina, *Phys. Rev. B* **67**, 094510 (2003).
  - [14] M. Tinkham, *Introduction to Superconductivity*, 2nd edition (McGraw-Hill, New York, 1996).